URN (Paper): urn:nbn:de:gbv:ilm1-2014iwk-071:9

58th ILMENAU SCIENTIFIC COLLOQUIUM
Technische Universität Ilmenau, 08 – 12 September 2014
URN: urn:nbn:de:gbv:ilm1-2014iwk:3

SELF-VOLUMETRIC ERROR COMPENSATION OF A MICRO-CMM

Kuang-Chao Fan[1,2], Shih-Hsin Hsu[1], Hao Zhou[2]

[1]Department of Mechanical Engineering, National Taiwan University, Taipei, Taiwan.
[2]School of Instrument Science and Opto-electronic Engineering, Hefei University of Technology, Hefei, China

ABSTRACT

This study proposes a self-volumetric error compensation approach to improve the volumetric accuracy of a developed Micro-CMM. The machine is built up by a co-planar stage for X and Y motions, a probe mounting spindle for Z motion and a touch-scanning probe. The co-planar stage is designed conforming to Abbe principle with displacement reading by laser interferometer and two angular sensors by autocollimator in each axis. The Z motion is detected by a linear grating interferometer. With prior calibration of static error terms, such as squareness errors, mirror form errors, and vertical straightness errors, the volumetric error can be self-calibrated by the installed sensors. A miniature Michelson interferometer with self-wavelength correction is developed to be a high precision linear sensor for limited space. Theoretical analyses are described. Experimental results validate the effectiveness of the developed system.

Index Terms **–** micro-CMM, volumetric error, Abbe principle, self-compensation

1. INTRODUCTION

Demands for measurement of three-dimensional (3D) micro-geometries over a large area have increased in the various industrial sectors [1, 2]. Due to the development of nanotechnologies, semiconductor, precision machinery, biological engineering, photovoltaic systems, etc., parts are toward the tiny and precision directions [3, 4]. The measurement accuracy for small parts has led to the development of precision manufacturing and inspection techniques to improve the quality and reliability of the product miniaturization. To face the inspection requirements of these micro parts, the development of small CMMs has become an interesting topic in recent years. During the past twenty years, a number of micro/nano-CMMs have been developed, for example, [5-10]. A micro/nano-CMM should possess extreme specifications, such as resolution to 1 nm, accuracy and repeatability to nanometer scales. Its accuracy calibration is a challenging task. In fact, there is no standard artifact that can be used to calibrate a micro/nano-CMM so far.

This study proposes a self-volumetric error compensation approach to improve the volumetric accuracy of a developed Micro-CMM. Theoretical analyses are described. Experimental results validate the effectiveness of the developed system. Detailed expressions are in the following sections.

2. STRUCTURAL DESIGN OF THE MICRO-CMM

The configuration of the Micro-CMM, as shown in Figure 1, comprises an XY co-planar stage mechanism, a Z-axis mechanism with counterweight mechanism and pagoda column in symmetric structure [10]. The co-planar stage is defined that X and Y motions are along the same common base plane, which is scraped and polished to allow lubrication for sliding contact. Each axis is driven by an ultrasonic motor to achieve long-stroke and nano-positioning motion [11]. The Z-motion is detected by the linear diffraction grating interferometer to nanometer resolution [12]. The X and Y motions are measured by the newly designed multi-degree-of-freedom measurement system (MDFMS), which includes a wavelength corrected Michelson interferometer and a dual-axis autocollimator for nanometer resolution and Abbe error compensation in Z-direction. Details of each part are described in the followings.

2.1 The Co-planar XY stage

The present study proposes a XY co-planar Abbe-free stage. As shown in Figure 2, it is a symmetrical structure for the X and Y motions. One side of each axis has an extension arm support by a linear stage, which is guided by a linear slide (THK Co. model SRS9N) and moved by an ultrasonic motor (Nanomotion Co. model HR4) mounted on the base plate. The other side of the moving table is equipped with a MDFMS for position, pitch and yaw feedback. The moving table slides over a common base plane, which is precisely ground to a flatness of less than 1 μm and isolated from the drive and sensing blocks. In order to ensure a smooth motion of the table, concave grooves are formed on the base plane using a scraping process and are filled with liquid lubricant to minimize the sliding friction force between the moving table and the base plane. This central table is moved in push-pull type driven by the ultrasonic motors and the extension arms.

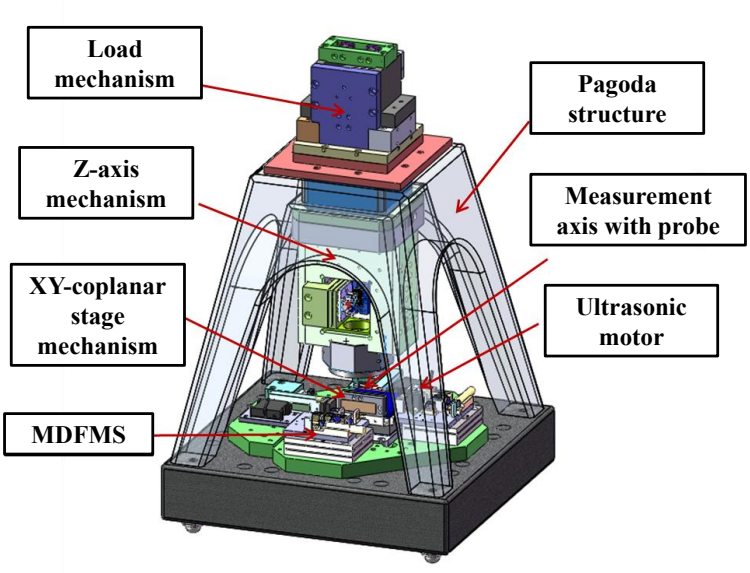

Fig. 1 The configuration of the Micro-CMM

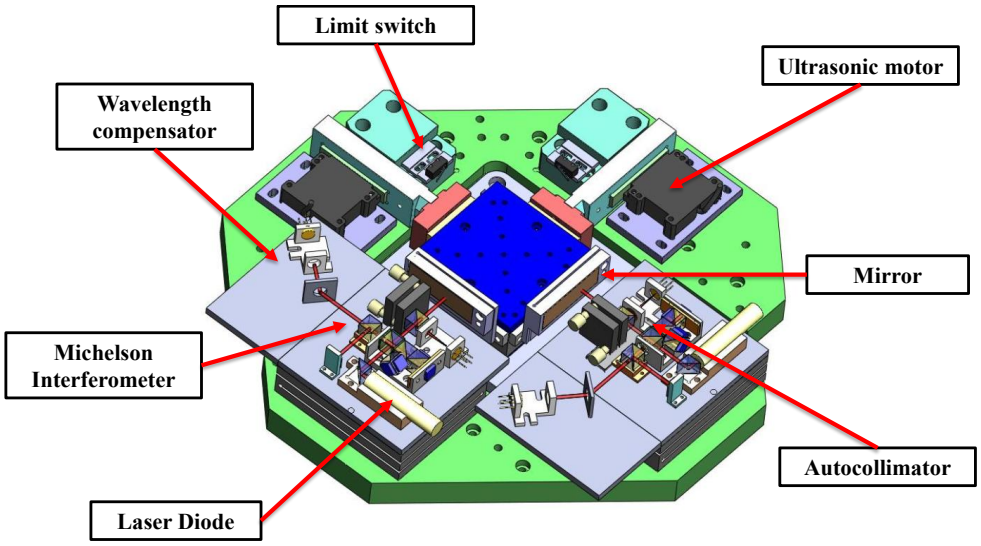

Fig. 2 The structure of XY co-planar stage

2.2 The Multi-Degrees-of-freedom measurement system

The configuration of the proposed optical system, named by multi-degree-of-freedom measurement system (MDFMS), is illustrated in Figure 3. The MDFMS contains one polarizing Michelson interferometer for displacement sensing and one dual axis autocollimator for pitch and yaw errors sensing. In the part of polarizing Michelson interferometer, a partially polarized laser beam of 635 nm wavelength from the laser diode LD impinges on the polarizing beam splitter PBS1 and is split into two beams: the transmitted P-beam and the reflected S-beam. The reflected beam is reflected by the reference mirror, and the transmitting is reflected by the moving mirror mounted on the stage. The displacement of the moving mirror will cause the optical path difference between the two reflected beams so as to produce interference. The quarter waveplates Q1 and Q2 prevent the reflected beams from going back into the laser diode, because each polarization state will be changed by 90º after passing a quarter waveplate twice. The two reflected beams are combined at PBS1 and converted into left and right circularly polarized beams by Q3. With the phase shift module composed by NPBS, PBS2 and PBS3, the interference fringe with 90º phase shift can be detected by photo-detectors PD1 to PD4. The displacement (L) of the mirror is calculated by

$$L = (\lambda / 2)[N + (\phi_o + \phi_f) / 2\pi] \tag{1}$$

where, λ is the wavelength of the laser diode, N is the number of pulse counts of interference signals, ϕ_o and ϕ_f are the initial and final phase angles of interference, respectively.

In front of the polarizing Michelson interferometer there is an autocollimator to measure the pitch and yaw motions of the moving mirror. According to the principle of optical autocollimator as shown in Figure 4, the tilted angle (θ) of the plane mirror will result in the focused spot being shifted laterally by $2f\theta$, where f is the focal length of the focusing lens. The built-in four-quadrant photodiode is used as the beam spot position detector to detect the amount of spot shift. The two tilted angles of the plane mirror can then be calculated.

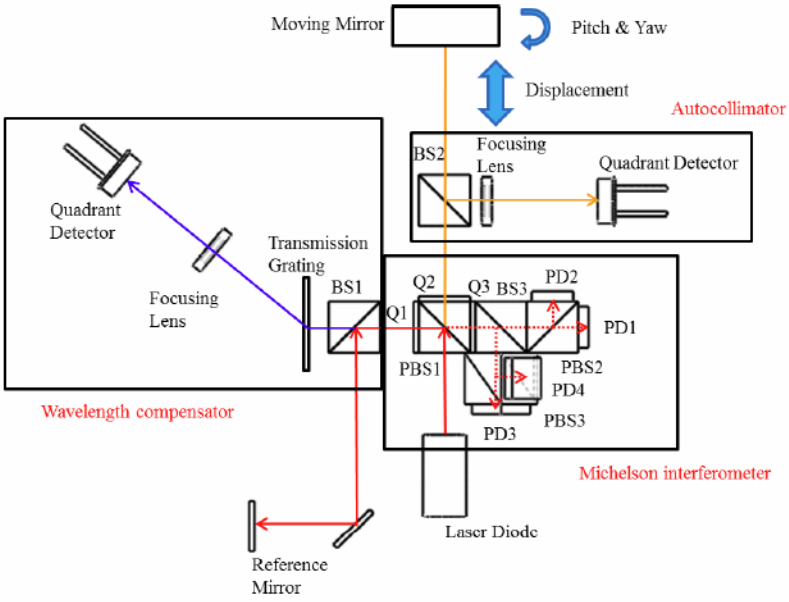

Fig. 3 The configuration of MDFM system

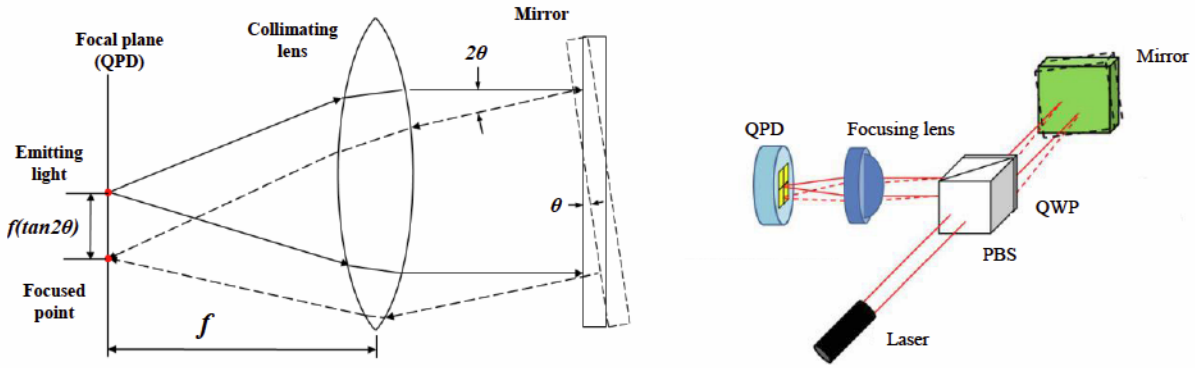

Fig. 4 The principle (left) and the optical configuration of autocollimator

2.3 Wavelength correction

In any laser interferometer the wavelength is the basic unit of length measurement. Common methods adopt various frequency stabilization techniques in order to stabilize the wavelength. However, for the He-Ne laser interferometer, the size is too large for micro-CMM; for the diode laser interferometer, the external cavity stabilization system is too complicate. Therefore, this study decided to develop an innovative wavelength correction method based on the spectral technique. As seen in Figure 3, the laser wavelength can be expressed by the following diffraction equation

$$\lambda'_{(\Delta\theta,T)} = d_0(1-\alpha\,(25-T))\,(\sin\theta_i + \sin(\theta_0+\Delta\theta)) \qquad (2)$$

Where, θ_i and θ_0 are the incident and $+1^{st}$ diffraction angles of the laser when it passes through a grating film (made of polyester by Edmund Optics), which has the specified grating pitch d_0 (= 1000 nm) at temperature 25 °C, α is the thermal coefficient of the grating film (= 1.7×10^{-5} /°C), $\Delta\theta$ is the measured change of diffraction angle due to the instantaneous temperature T and λ' is the real-time wavelength of the laser. In experiments, we adopted the SIOS-1000 laser interferometer as the reference because of its small head that can be installed in the micro-CMM chamber. At each different temperature, we calibrated the wavelength of

the laser diode by comparing a 20 mm distance with SIOS-1000. Applying the optimization technique of MATLAB, the setting values of θ_i and θ_0 can be obtained ($\theta_i = -1.9°$ and $\theta_0 = 41.76°$). Since d_0 and α are already known, we can easily calculate corrected wavelength from Eq. (2) if T and $\Delta\theta$ are measured.

2.4 The probe system

A high precision contact probe for a micro/nano-CMM was developed to detect the 3D motion of the stylus tip. This con brations with a nano measuring and positioning machine (NMM) proved that the typical standard deviation was less than 20 nm for both the trigger and scanning modes [13].

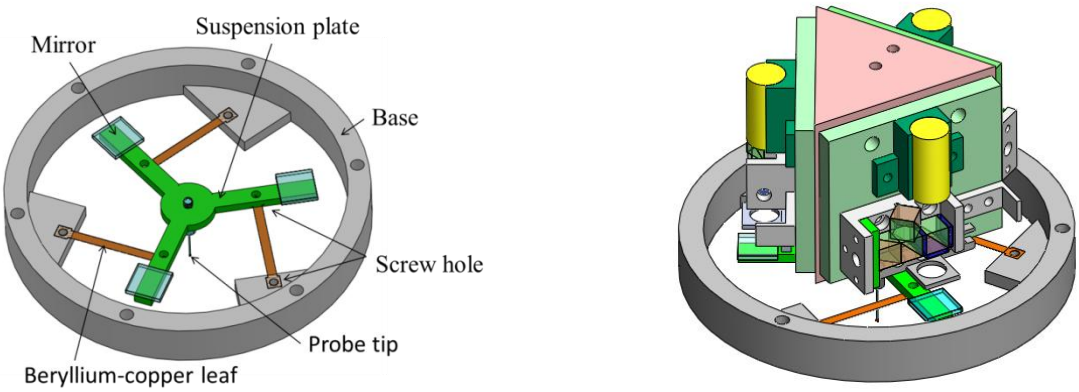

Fig. 5 The probe system, (left) floating pplte and (right) with three Michelson interferometers

3. SELF-VOLUMETRIC ERROR COMPENSATION

As expressed in the previous section, this pagoda type micro-CMM is mainly composed of two modules, namely a high-precision co-planar stage mounted onto a granite table and a high-precision Z-stage equipped with a high-precision contact scanning probe. The volumetric error analysis and compensation can be divided into 2-D and 3-D models. Wave

3.1 The 2-D space

In 2-D space, the error model of XY co-planar stage is studied. In each axis, the MDFMS detects the displacement and two angular motions of the long mirror (LM) in real-time. In addition to the geometric errors of each axis, the straightness of each LM (called form error) will also cause measurement errors. Figure 6 shows the possible motion errors.

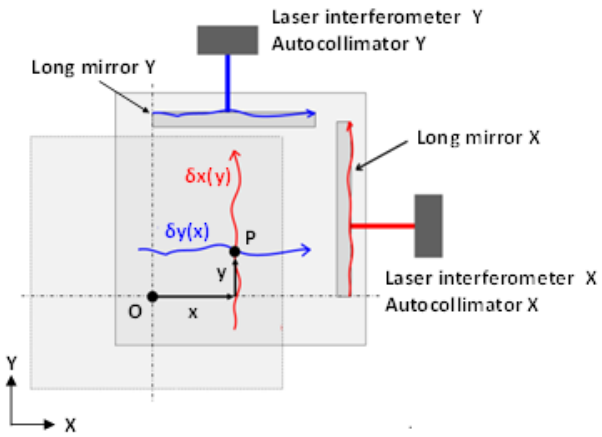

Fig. 6 Straightness errors and mirror errors of the co-planar stage

The readings of X-laser interferometer $L_x(x, y)$ and Y-laser interferometer $L_y(x, y)$ contain some error sources, expressed by

$$L_X(x,y) = x + \delta_x(y) + M_x(y) - y\gamma_{xy} + \Delta L_x(pitch, yaw) \quad (3)$$

$$L_y(x,y) = y + \delta_y(x) + M_y(x) + \Delta L_y(pitch, yaw) \quad (4)$$

where, $\delta_x(y)$ is the straightness error in X-direction when the stage is moved in Y-direction, $\delta_y(x)$ is the straightness error in X-direction when the stage is moved in Y-direction, $M_x(y)$ is the X-straightness error of Y-mirror, $M_y(x)$ is the Y-straightness error of X-mirror, γ_{xy} is the squareness error of X and Y motions, $\Delta L_x(pitch, yaw)$ and $\Delta L_y(pitch, yaw)$ are the pitch and yaw induced optical path errors of the linear interferometers in X and Y directions, respectively, and x and y are the actual displacements of the co-planar stage. From these two equations, it can be seen that the straightness and squareness errors of $\delta_x(y)$, $\delta_y(x)$ and γ_{xy} can be automatically compensated by the two MDFM systems. Considering that the stage is a rigid body, the yaw angle read by X-autocollimator and Y-autocollimator should be the same. The difference should be due to the straightness of the mirror. Therefore, the following relationship should exist.

$$M_y(x) = \int [\varepsilon_z(y) - \varepsilon_z(x)]dx \quad (5)$$

$$M_x(y) = \int [\varepsilon_z(x) - \varepsilon_z(y)]dy \quad (6)$$

where, $\varepsilon_z(x)$ is the yaw angle read by X-autocollimator and $\varepsilon_z(y)$ is the yaw angle read by Y-autocollimator. The mirror error is a static term that is only related to the current stage position. The stage has a home position, detected by a home sensor. The X and Y position of the stage is considered as the absolute position from the origin (home). The mirror error can thus be calibrated in advance and compensated in equations (3) and (4). Fig. 7 is the measured Δyaw (=$\varepsilon_z(y) - \varepsilon_z(x)$) along the X motion. The straightness error of mirror Y ($M_y(x)$) is shown in Figure 8. It is about 200 nm with quite good repeatability at different Y positions.

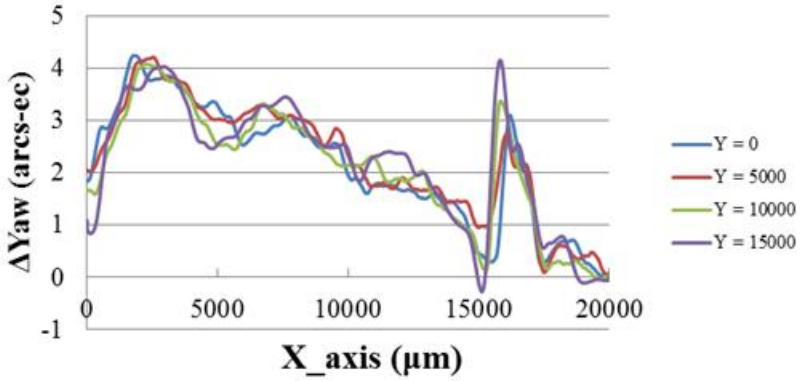

Fig. 7 Difference in yaw readings along X-motion

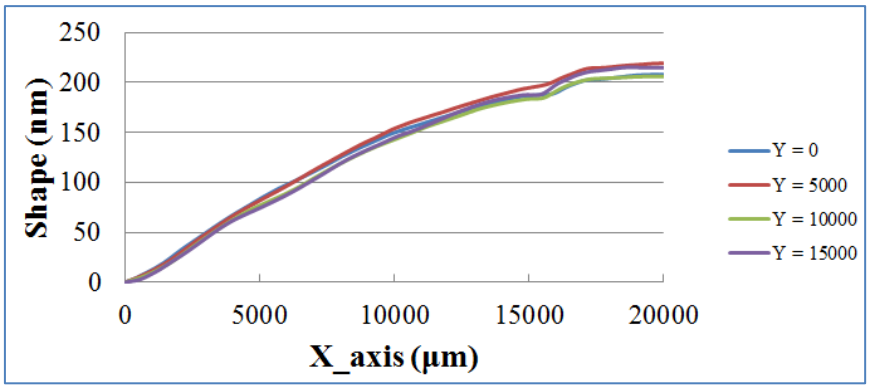

Fig. 8 Measured straightness (form) error of mirror Y

The last term in Eq. (3) or (4) is the induced optical path difference of the laser interferometer system due to pitch and yaw of the moving LM. From experiments, the maximum angular error is about 20 arc-sec and the maximum moving distance is about 20 mm. In practice, the induced $\Delta L_x(pitch, yaw)$ or $\Delta L_y(pitch, yaw)$ is less than 1 nm and is negligible.

Hence, in 2-D space, the actual coordinate of the moving co-planar stage conforms to Abbe principle and is the laser reading self-compensated by the mirror's form error only.

$$P_x = x + \delta_x(y) - y\gamma_{xy} = L_x(x, y) - M_x(y) \tag{7}$$

$$P_y = y + \delta_y(x) = L_y(x, y) - M_y(x) \tag{8}$$

3.2 The 3-D space

3.2.1 Determination of Abbe offset

In 3-D space, the probe motion in Z direction has to be considered that will generate Abbe offset in Z and Abbe errors in X and Y at the probing position. The amount of Abbe offset at any Z position can be obtained from experiments. Figure 9 shows the schematic diagram of the experimental procedure. Firstly, we define the length (H) between gauge and quadrant detector (QPD). Secondly, a QPD is employed to assist the optical alignment so that the laser beam can be adjusted to allow projecting onto the detector at the same position both at near end and far end of travel. Thirdly, through the positioning experiment, pitch deviations (ε_Y) of the motion stage will be measured by MDFMS. According to positioning error (E_X), the corresponding Abbe offset (Lz) will be obtained by equation (9). Fourthly, moving the Z-axis until the probe touch the gauge and get the trigger signal as the position P. Fifthly, in order to move the probe to the center of QPD, the Z-axis need to move the distance (H-r) due to the probe radius (r). Finally, the Abbe offset will be obtained when probe is under the position H.

$$E_X = \varepsilon_Y \cdot L_Z \tag{9}$$

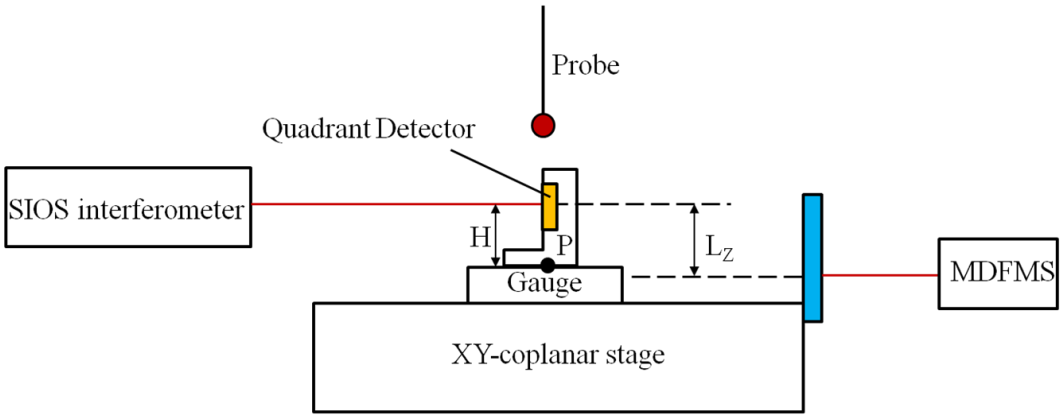

Fig. 9 Experiment for Abbe offset finding

3.2.2 Volumetric error compensation

When the probing point is at the space point P, its coordinates (P_x, P_y, P_z) are expressed by the following equations.

$$\mathrm{P}_x(x,y,z) = x + \delta_x(y) + \delta_x(z) + M_x(y) - y\gamma_{xy} + z\gamma_{xz} + Z_{abbe} \times \varepsilon_y(x) \quad (10)$$

$$\mathrm{P}_y(x,y,z) = y + \delta_y(x) + \delta_y(z) + M_x(y) - z\gamma_{yz} + Z_{abbe} \times \varepsilon_x(y) \quad (11)$$

$$\mathrm{P}_z(x,y,z) = z + \delta_z(x) + \delta_z(y) \quad (12)$$

Where, γ_{xy} and γ_{xz} are the squareness errors of X-Y axes and X-Z axes, respectively, Z_{abbe} is the Abbe offset. Substituting (7) and (8) into (10) to (12) yields

$$\mathrm{P}_x(x,y,z) = L_x(x,y) - M_x(y) + Z_{abbe}(\gamma_{xz} + \varepsilon_y(x)) \quad (13)$$

$$\mathrm{P}_y(x,y,z) = L_y(x,y) - M_y(x) + Z_{abbe}(\gamma_{yz} + \varepsilon_x(y)) \quad (14)$$

$$\mathrm{P}_z(x,y,z) = L_z(z) + \delta_z(x) + \delta_z(y) = L_z(z) + \delta_z(x,y) \quad (15)$$

The squareness errors (γ_{xy} and γ_{xz}) are static terms that can be calibrated using laser and optical square. The straightness error in Z direction during X and Y motions of the co-planar stage, $\delta_z(x,y)$, can also be calibrated in advance using a precision optical flat. The mirror form errors can be obtained by Eqs. (5) and (6). Therefore, the volumetric error can be self-compensated by

$$\Delta\,\mathrm{Ex} = \mathrm{P}_x(x,y,z) - L_x(x,y) = -M_x(y) + Z_{abbe}(\gamma_{xz} + \varepsilon_y(x)) \quad (13)$$

$$\Delta\,\mathrm{Ey} = \mathrm{P}_y(x,y,z) - L_y(x,y) = -M_y(x) + Z_{abbe}(\gamma_{yz} + \varepsilon_x(y)) \quad (14)$$

$$\Delta\,\mathrm{Ez} = \mathrm{P}_z(x,y,z) - L_z(z) = \delta_z(x,y) \quad (15)$$

4. EXPERIMENTS

Some experiments have been conducted to validate the effectiveness of the developed self-volumetric error compensation method.

4.1 Wavelength correction results

The exact wavelength of the laser is calculated from Eq. (2) with the measured values of ambient temperature T and the change of diffraction angle ($\Delta\theta$). A comparison was made with a SIOS laser interferometer for a certain amount of distance measurement. Table 1 lists three times of experiments. The calibrated wavelength is calculated from actual SIOS displacement divided by total phase angle change, as given in Eq. (1). The corrected wavelength is the exact self-corrected value of the Michelson interferometer, as given in Eq. (2). The relative error of the self-corrected wavelength is all about the order of 10^{-6}. In other words, for a moving distance of 15 mm the maximum displacement error of the Michelson interferometer would be less than 15 nm. For a low cost system, this is an acceptable error range.

Table 1 Comparison results of wavelength correction method

Times	Calibrated wavelength (nm)	Corrected wavelength (nm)	Error (nm)	Δλ/λ (%)
1	632.8199	632.8222	0.0023	3.60544E-06
2	632.8240	632.8195	0.0045	7.15929E-06
3	632.8173	632.8118	0.0055	8.75114E-06

4.2 Abbe error compensation results

As explained in section 3.2.1, the micro-CMM system can detect the Abbe offset in Z and pitch errors of the co-planar stage. The Abbe errors occurred to X and Y laser interferometer readings can be self-compensated according to Eq. (9). Figure 10 shows an example of before and after Abbe error compensation. The positioning error for a 20 mm distance can be controlled to within ±20 nm after compensation.

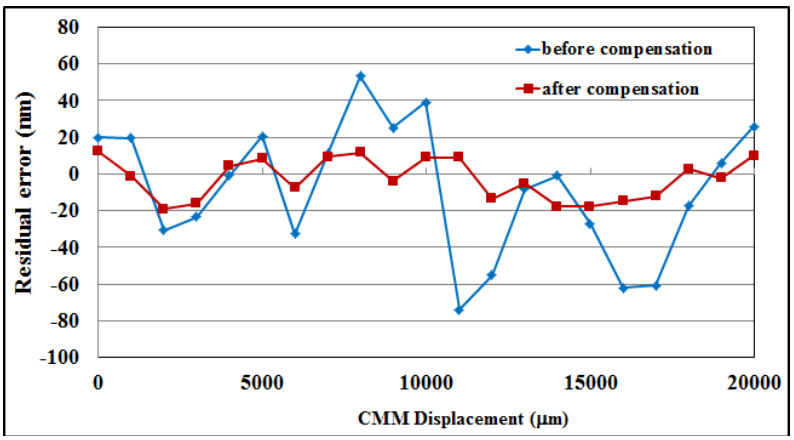

Fig. 10 Results of with and without Abbe error compensation

5. CONCLUDING REMARKS

A pagoda type micro-CMM with MDFMS in X and Y axes of the co-planar stage, and a grating interferometer in Z axis has been developed. On this machine, a self-volumetric error compensation scheme has been proposed. Theoretical analysis shows that if the static terms of geometric errors can be calibrated in advance, the rest dynamic errors can be directly measured by the MDFMS. The self-volumetric error compensation could thus be made possible. Comparison with a commercial laser interferometer (SIOS 1000), experimental results validate the effectiveness of the proposed method.

REFERENCES

[1] T.V. Vorburger, J.A. Dagata, G. Wikeniging, and K. Iizuka, "Industrial uses of STM and AFM," CIRP Annals – Manufacturing Technology, Vol. 46, pp.597–620, 1997.

[2] M. Michihata, Y. Takaya, and T. Hayashi, "Development of the nano-probe system based on the laser-trapping technique," CIRP Annals – Manufacturing Technology, Vol. 49, pp. 493–496, 2008.

[3] P. Mckeown, "Nanotechnology-special article," Proc. of Nano-metrology in Precision Engineering, pp. 5–55, 1998.

[4] H.N. Hansen, et al, "Dimensional micro and nano metrology," CIRP Annals – Manufacturing Technology, Vol. 55(2), pp. 721-743, 2006.

[5] K. Takamasu, R. Furutani, and S. Ozono, "Development of nano-CMM," Proceedings of XIV IMEKO World Congress, Finland, pp. 34-39, 1997.

[6] G.N. Peggs, A.J. Lewis, and S. Oldfield, "Design for a compact high-accuracy CMM," CIRP Annals - Manufacturing Technology, Vol. 48(1), pp. 417-420, 1999.

[7] M.M.P.A. Vermeulen, P.C.J.N. Rosielle, and P.H.J. Schellekens, "Design of a high-precision 3D-Coordinate Measuring Machin," CIRP Annals - Manufacturing Technology, Vol. 47(1), pp. 447-450, 1998.

[8] A. Küng, F. Meli, and R. Thalmann, "Ultraprecision micro-CMM using a low force 3D touch probe," Measurement Science and Technology, Vol. 18(2), pp. 319, 2007.

[9] J. Jäger, E. Manske, et al, "Nanopositioning and -Measuring Technique," 7th International Symposium on Laser Metrology, Novosibirsk, Russia, Vol. 4900, P755-762, 2002.

[10] K.C. Fan, F. Cheng, H.Y. Wang, and J. K. Ye, "The system and the mechatronics of a pagoda type micro-CMM," Int. J. of Nanomanufacturing (IJNM), Vol. 8, No. 1/2, pp. 67-86, 2012.

[11] H.Y. Wang, K.C. Fan, J.K. Ye, and C.H. Lin, "A long-stroke nano-positioning control system of the co-planar stage," IEEE/ASME Transactions on Mechatronics, Vol. 19, No. 1, pp.248-356, 2014.

[12] F. Cheng, and K.C. Fan, "A linear diffraction grating interferometer with high alignment tolerance and high accuracy," Applied Optics, Vol. 50, No. 22, pp. 4550-4556, 2011.

[13] C.M. Huang, B.H. Liao, and K.C. Fan, "A contact probe using Michelson interferometer for CMM," Proc. ISPEMI2012, Chengdu, China, Aug. 9-11, 2012.

CONTACT

Prof. Kuang-Chao Fan fan@ntu.edu.tw